Supporting Information

A Polyoxovanadate-Based Metal-Organic Framework Unlocks the Potential for Advanced Calcium-Ion Storage

Yiran Cao,[#,a,b,] Lixiao Xiang,[#,a] Wei Wei,[a] Wenhua Yang,[a] Zhe Li,[a] Haoyu Wu,[a] Jie Xu,[a] Xia Wang,[*,a] Jikun Li,[*,c] and Ying Xiao*[,b]

a. College of Physics, University-Industry Joint Center for Ocean Observation and Broadband Communication, Qingdao University, Qingdao 266071, P. R. China.
E-mail: wangxiakuaile@qdu.edu.cn.
b. State Key Laboratory of Chemical Resource Engineering, Beijing Key Laboratory of Electrochemical Process and Technology for Materials, National Engineering Research Center for Fuel Cell and Hydrogen Source Technology, Beijing University of Chemical Technology, Beijing 100029, P. R. China. E-mail: yxiao@buct.edu.cn
c. College of Chemistry and Chemical Engineering, Taishan University, Tai'an 271021, P. R. China. E-mail:lijk0212@163.com.

Experimental section

(1) Synthesis of Co,V-POM@GO

Firstly, $[Co_3(4\text{-}NH_2\text{-}trz))_6][V_6O_{18}]\cdot 3H_2O$ (Co,V-POM) was synthesized by the previous report.[s1] Subsequently, it was mixed with GO with a mass ratio of 1:2 under ultrasound for 24h. Finally, the product was obtained after cleaning and freeze-drying.

(2) Material characterization

The morphologies of the final product were characterized by scanning electron microscopy (SEM, JSM-6700F, JEOL) and transmission electron microscopy (TEM, Tecnai G2 F30, FEI). X-ray photoelectron spectroscope (XPS, Thermo ESCALAB 250Xi) was utilized to analyze the surface elemental composition and valence.

(3) Electrochemical tests

The positive electrode was composed of Co,V-POM@GO (70 wt%), Ketjen Black (20 wt%) and polyvinylidene fluoride (PVDF 10 wt%), which were mixed and dispersed in methyl-2-pyrrolidinone (NMP) and ground evenly. The slurry was coated on aluminum foil and dried in a vacuum drying oven at 60° for 12 h. The loading mass of active materials is about 0.6~1.2 mg cm^{-2}. Finally, the CR2032 coin cells were assembled in an argon-filled glovebox with Whatman glass microfiber filter (GF/A) as the separator, ACC (1500-2500 m^2g^{-1}, GUN EI Chemical Industry Co. Ltd) as the counter electrode and 0.8 M $Ca(TFSI)_2$ dissolved in a mixture of ethylene carbonate (EC), dimethyl carbonate (DMC), propylene carbonate (PC), ethylmethyl carbonate (EMC) (vol/vol/vol/vol=2:3:2:3) as the electrolyte. Galvanostatic charge/discharge measurement was conducted with a multi-channel battery testing system (Neware CT-4008T-5V20 mA-164, Shenzhen, China). Cyclic voltammetry (CV) tests were carried out using an electrochemical workstation (CHI660E).

(4) Theoretical calculations

In this work, all structural models are fully subjected to density-functional theory (DFT) calculations using the ultra-soft pseudopotential (USP) from the CASTEP package, and the exchange and correlation energies are treated using the generalised gradient approximation (GGA) of the Perdew-Burke-Ernzerhof (PBE) generalisation. The electronic wave function is expanded using a plane wave basis group with a cut-off energy of 340 eV. A Monkhorst-Pack Brillouin lattice of $2\pi \times 0.04$ A^{-1} was used for all calculations, with a convergence value of 0.02 meV/atom for the total energy and 0.05 eV/Å for the atom. Three possible locations for calcium ion adsorption in Co,V-POM@GO, two possible diffusion paths, and a number of other possible routes for the calcium ion adsorption in Co,V-POM@GO were calculated. The diffusion barriers of calcium ions in Co,V-POM@GO were calculated by the periodic LST/QST method in CASTEP.

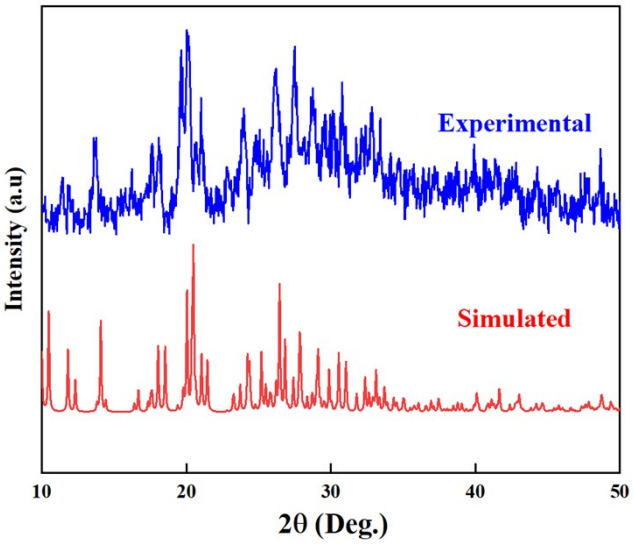

Fig. S1 XRD patterns of Co, V-POMOF@GO.

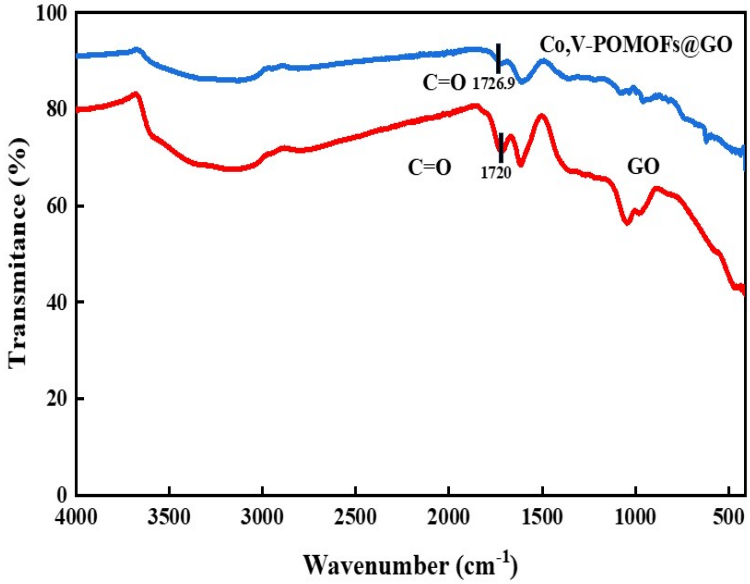

Fig. S2 FTIR spectra of GO and Co, V-POMOFs@GO.

It can be seen that that the characteristic peak of the C=O stretching vibration in GO shifts from 1720 cm-1 to 1726.9 cm-1 upon complexation with Co, V-POMOFs.This shift indicates a strong interaction between the oxygen-containing functional groups on the GO surface (specifically the carboxyl groups) and the metal centers (Co/V) of the POMOFs, confirming the successful functionalization of GO with the POMOFs .

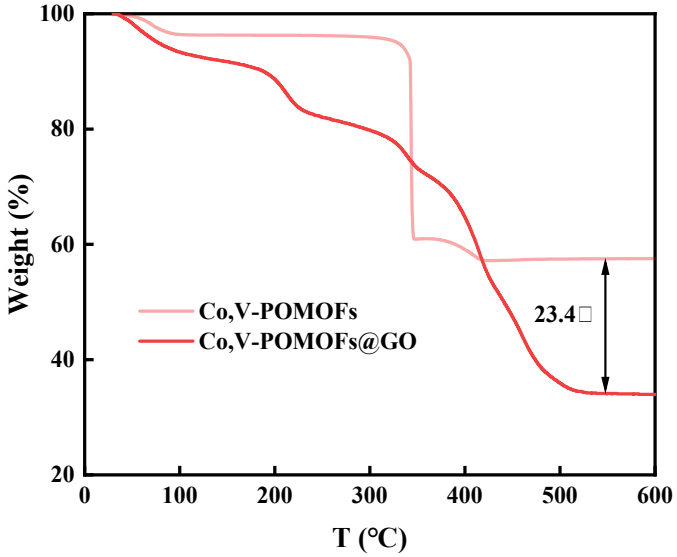

Fig. S3 TGA curves of Co,V-POMOFs and Co,V-POMOFs@GO.

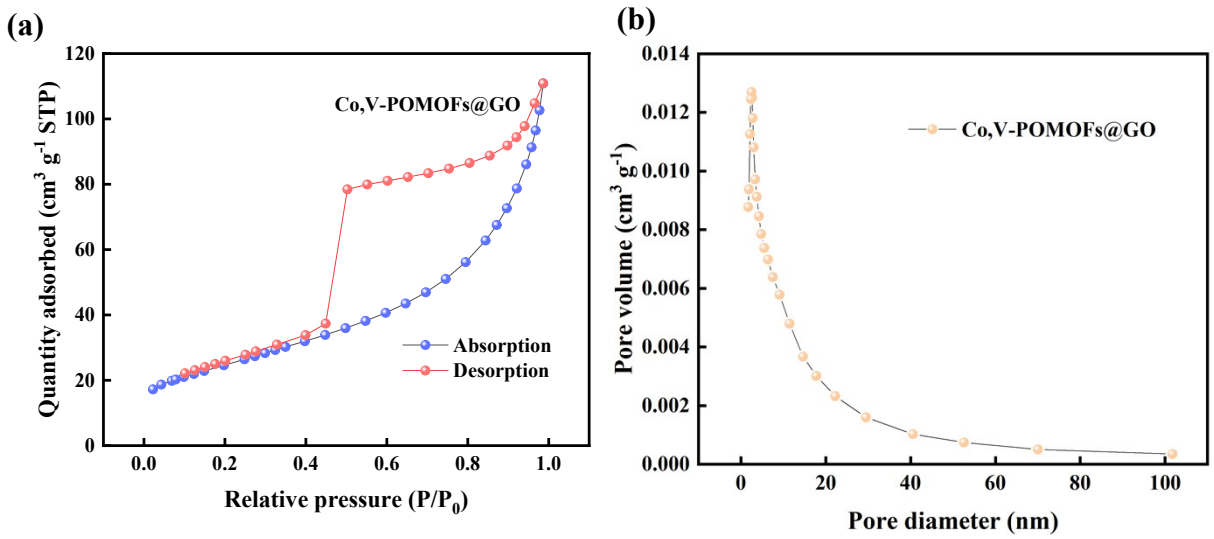

Fig. S4 (a) N_2 adsorption-desorption isotherms and (b) The pore size distribution curves of Co,V-POMOFs@GO.

Co,V-POMOFs@GO exhibits a Type IV nitrogen isotherm with a broad hysteresis loop in the pressure range of 0.4-1.0 (P/P0), which implies the existence of mesopores. Simultaneously, the pore size distribution plot presents that Co,V-POMOFs@GO possesses a relatively wide pore size distribution with an average pore size of approximately 7.74 nm. Furthermore, the Brunauer-Emmett-Teller (BET) specific surface area of Co,V-POMOFs@GO was calculated to be around 88.60 $m^2 g^{-1}$ (Fig. S4).

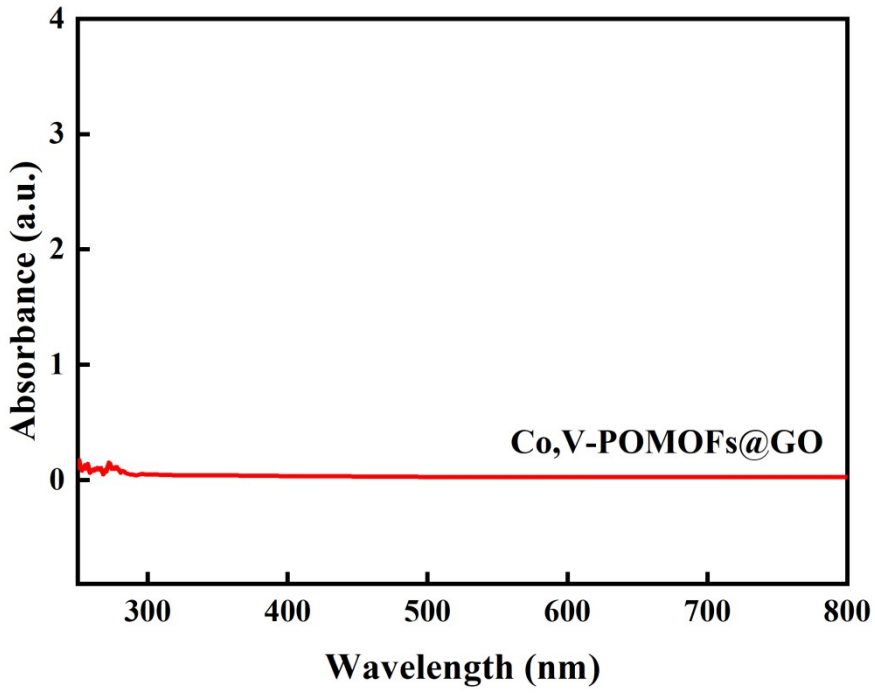

Fig. S5 UV-Vis absorption spectrum of the electrolyte after the immersion of Co,V-POMOFs@GO.

The aluminum foil with Co,V-POMOFs@GO was left to stand in the electrolyte for 24 hours. Ultraviolet-visible (UV-Vis) spectroscopy was performed on the supernatant (Fig. S6). It was found that there were almost no characteristic peaks in the electrolyte, which confirms that Co,V-POMOFs@GO delivers good stability in the electrolyte.

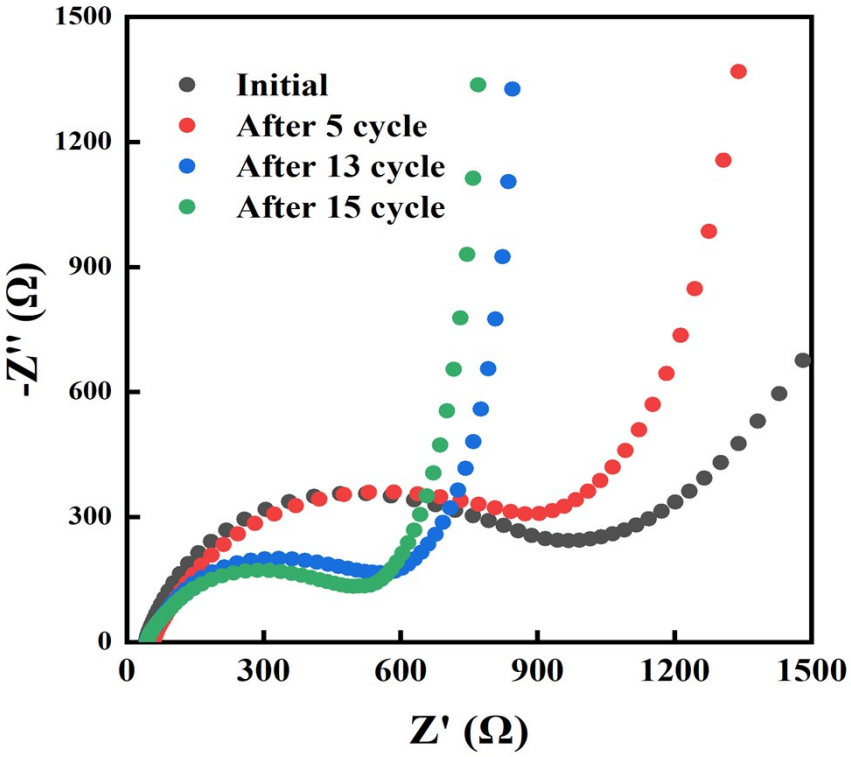

Fig. S6. EIS spectra of Co,V-POMOFs@GO after different cycles.

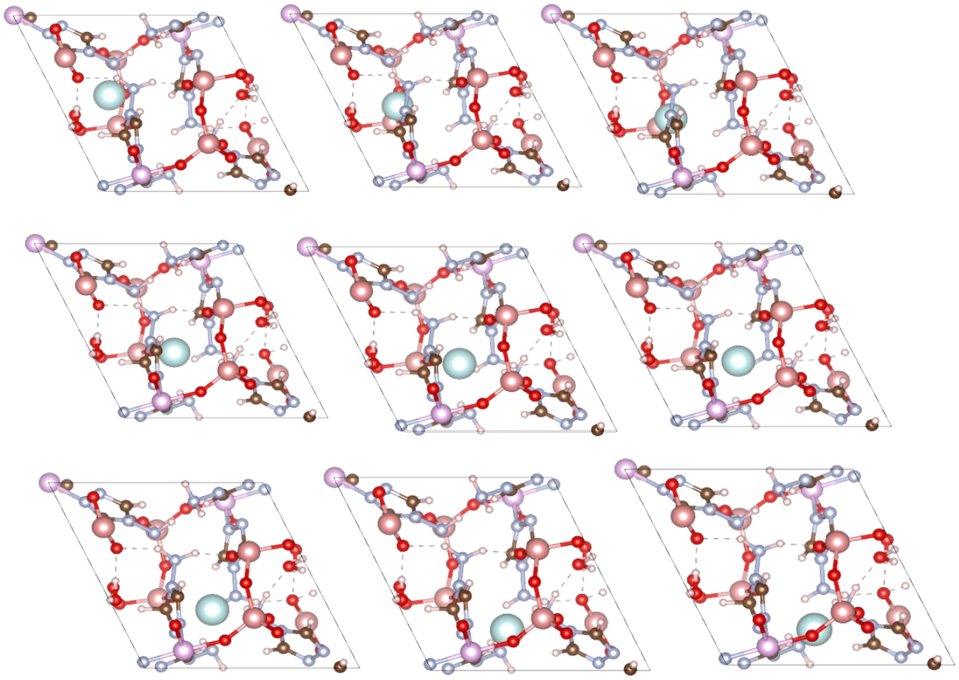

Fig. S7. Schematic diagram of the Ca^{2+} diffusion steps from pore 1 to pore 2 in Co,V-POMOFs@GO.

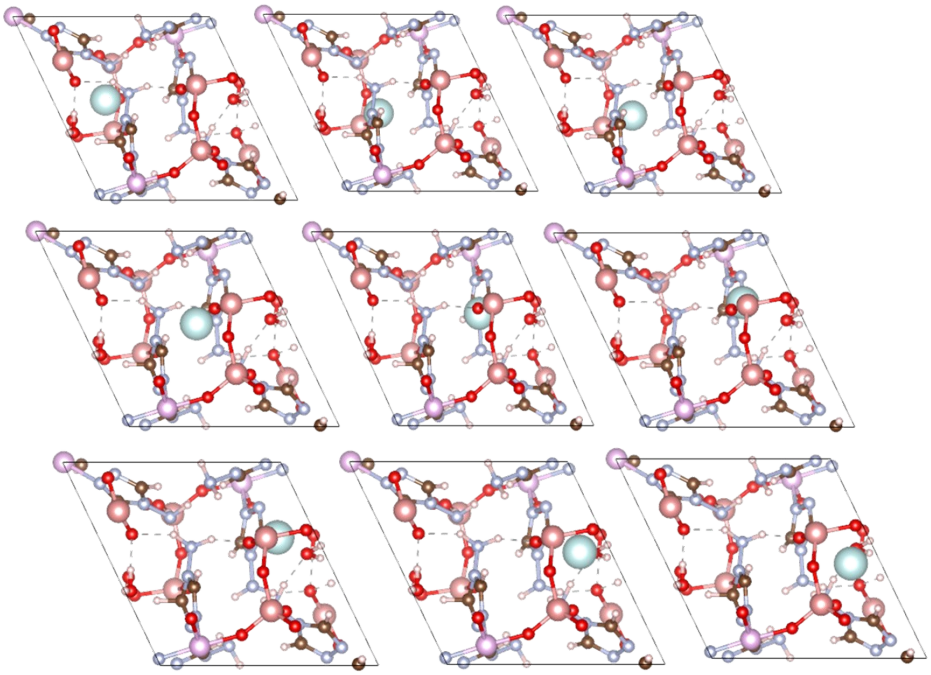

Fig. S8. Schematic diagram of the Ca^{2+} diffusion steps from pore 1 to pore 3 in Co,V-POMOFs@GO.

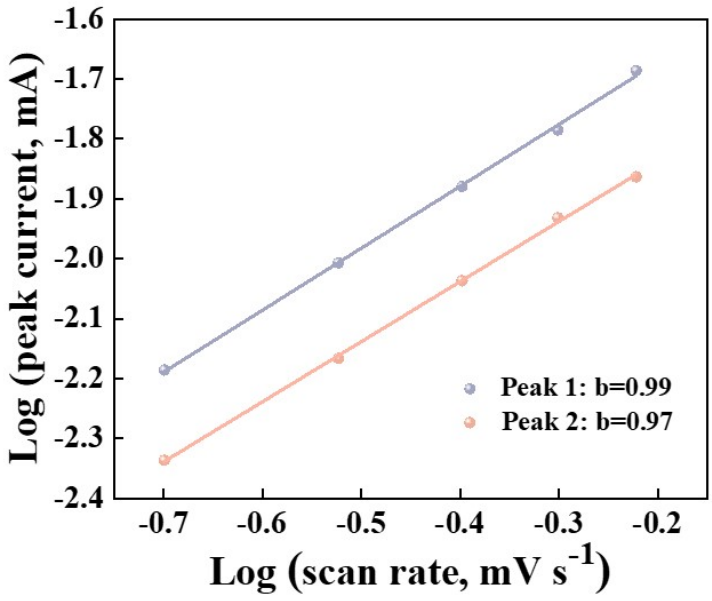

Fig. S9 Plots of log(*i*) vs. log(*v*) for the two redox peaks in the CV curves of Co, V-POMOF@GO.

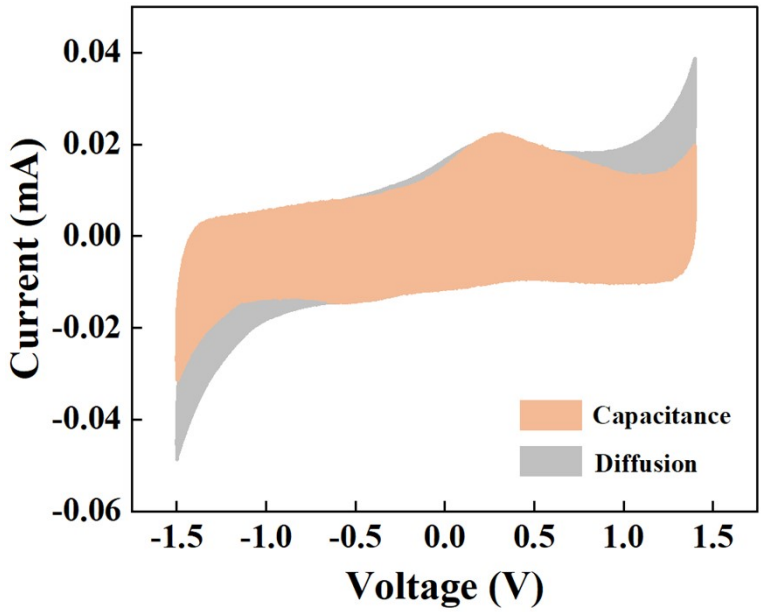

Fig. S10 Pseudocapacitive contribution region (shaded in orange) at a scan rate of 0.8 mV s^{-1} of Co, V-POMOF@GO.

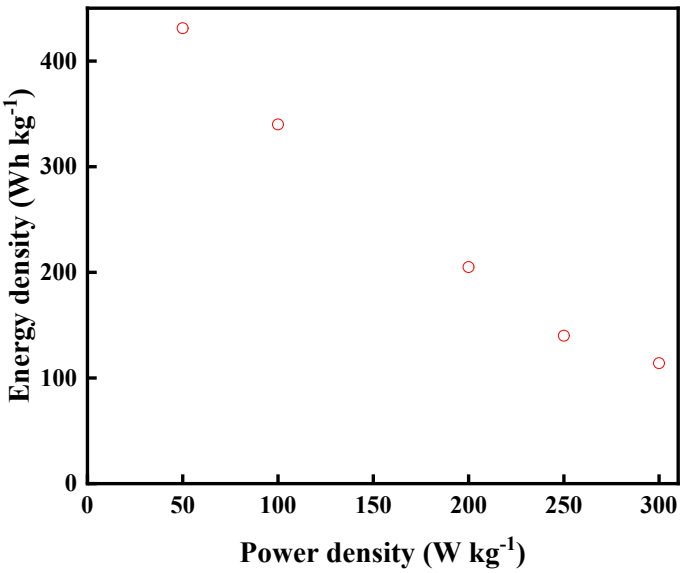

Fig. S11 Ragone plot of Co,V-POMOFs@GO.

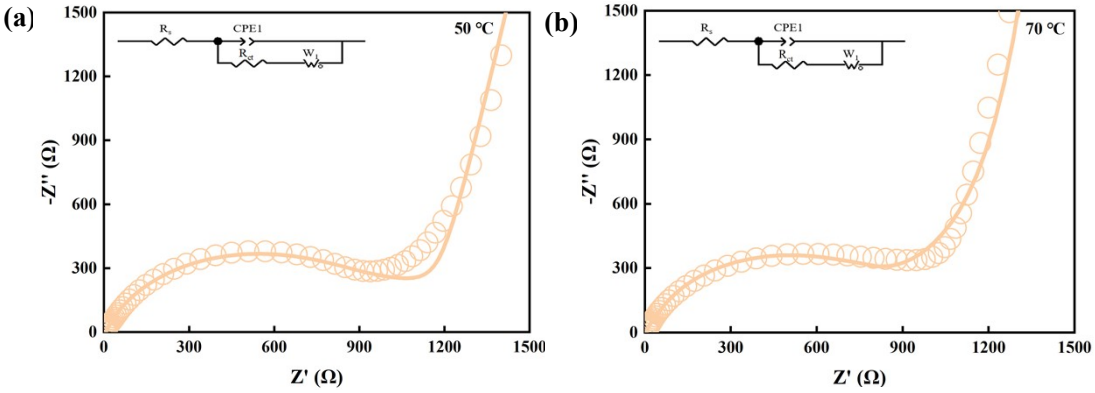

Fig.S12 Nyquist and fitted plots of Co,V-POMOFs@GO at 50 and 70 ºC.

Table S1. Calcium storage performance of this work vs. literature data.

Cathode materials	Reversible capacity (mAh g^{-1})	Current density (mA g^{-1})	Capacity retention	References
Co,V-POMOFs@GO	320.45	50	96.7%	This work
$VOPO_4 \cdot 2H_2O$	100	20	86%	6
δ-MnO_2	125	100	53.6%	11
$BaV_6O_{16} \cdot 3H_2O$@GO	339.45	50	84%	32
$K_2V_6O_{16} \cdot 2.7H_2O$	94	50	78.3%	33
$CaV_6O_{16} \cdot 2.8H_2O$	131.7	50	94.4%	34
β-$Ag_{0.33}V_2O_5$	179	12.3	47%	35
MnO_2@PANI	150	100	91.9%	36
CuS/C	126	100	92%	37
$Ca_{0.28}V_2O_5 \cdot H_2O$	120	30	74%	38
$Ca_xNa_{0.5}VPO_{4.8}F_{0.7}$	65	66.6	92%	39
V_2O_5	150	50 (uA cm^{-2})	20%	40
$Ti_2O(PO_4)_2(H_2O)$	60.8	50	95%	41
VO_2(B)	120	100	79%	42

Table S2 Diffusion rate of calcium ions in positive electrode materials in the previous reports.

Cathode	Diffusion efficient ($cm^2 s^{-1}$)	References
VO_2(B)/rGO	7.51×10^{-12}	s2
NHVO-H@GO@CNT	5.52×10^{-1}-2.61×10^{-13}	s3
β-$Ca_{0.14}V_2O_5$	$10^{-7.7}$-$10^{-8.7}$	s4
$CaV_6O_{16}\cdot2.8H_2O$	$7.5\times10^{-12}$$1.8\times10^{-13}$	s5
$BaV_6O_{16}\cdot3H_2O$@GO	2.3×10^{-1}-8.92×10^{-14}	s6
K_xVPO_4F	10^{-10}-10^{-11}	s7
$M_xV_2O_5\cdot nH_2O$, M=Ni, Co, Mn	NiVO:7.51×10^{-12} CoVO:1.32×10^{-14} MnVO:5.64×10^{-10}	s8
$Zn_{3-x}Cu_x(OH)_2V_2O_7\cdot2H_2O$	10^{-6}-10^{-14}	s9
Co,V-POMOFs@GO	**10^{-6}-10^{-10}**	This work

Table S3 R_{ct} values at different temperatures according to equivalent circuit model

T (°C)	R_{ct} (Ω)
30	1667
40	1429
50	1250
60	1110
70	990

s1. Y. Wang, Y. Wang, C. Sun, Z. Han, J. Li, J. Xu, J. Qin, H. Sun and X. Wang, *ACS Applied Materials & Interfaces*, 2025，**17**, 59235–59246.

s2. Y. Wang, J. Wang, W. Zhang, F. Chao, J. Li, Q. Kong, F. Qiao, L. Zhang, M. Huang and Q. An, *Advanced Functional Materials*, 2024, **34**, 2314761.

s3. J. Wang, Y. Zhang, F. Qiao, Y. Jiang, R. Yu, J. Li, S. Lee, Y. Dai, F. Guo and P. Jiang, *Advanced Materials*, 2024, **36**, 2403371.

s4. S. J. Richard Prabakar, A. B. Ikhe, W. B. Park, D. Ahn, K. S. Sohn and M. Pyo, *Advanced Functional Materials*, 2023, **33**, 2301399.

s5. J. Wang, J. Wang, Y. Jiang, F. Xiong, S. Tan, F. Qiao, J. Chen, Q. An and L. Mai, *Advanced Functional Materials*, 2022, **32**, 2113030.

s6. L. Xiang, W. Yang, Y. Wang, X. Sun, J. Xu, D. Cao, Q. Li, H. Li and X. Wang, *Chemical Communications*, 2024, **60**, 5459-5462.

s7. R. Li, Y. Lee, H. Lin, X. Che, X. Pu, Y. Yi, F. Chen, J. Yu, K. C. Chan and K. Y. Park, *Advanced Energy Materials*, 2024, **14**, 2302700.

s8. X. Zhao, L. Li, L. Zheng, L. Fan, Y. Yi, G. Zhang, C. Han and B. Li, *Advanced Functional Materials*, 2024, **34**, 2309753.

s9. J.-M. Cao, Y. Liu, K. Li, I. V. Zatovsky, J.-L. Yang, H.-H. Liu, Z.-Y. Gu, X. Gao, K.-Y. Zhang and S.-H. Zheng, *National Science Review*, 2025, **12**, nwaf074.